Some Estimates of Tunneling Splittings in Small Clusters

David J. Wales

Contribution from University Chemical Laboratories, Lensfield Road, Cambridge CB2 1EW, United Kingdom

Received May 17, 1993®

Abstract: A simple treatment is used to estimate the tunneling splittings caused by rearrangements in a variety of model cluster systems, including $(HF)_2$, benzene-Ar, benzene–Ar_2, $C_5H_5^+$, $B_8H_8^{2-}$, and homoatomic clusters bound by the Lennard–Jones and Morse potentials. Given sufficient generators to represent all the point group operations and feasible rearrangements, the effective molecular symmetry group is calculated along with the connectivity of the minima on the potential energy surface. This defines the secular determinant which provides the best solutions to the multiminima problem that may be written as linear combinations of localized functions. A Hückel-type approximation is then employed, assuming that the only non-zero off-diagonal Hamiltonian matrix elements are between minima which are directly linked by a rearrangement. The magnitude of this matrix element is estimated from properties of the calculated reaction pathways, using a model one-dimensional Schrödinger equation. Solving the Hückel-type secular equations gives the splitting pattern for each rigid-molecule energy level and also an estimate of the magnitude of the effect, along with the electric dipole allowed transitions. The results compare satisfactorily with experiment where data are available (i.e. the splittings are of the right order of magnitude), and a number of other cases are identified where tunneling effects might be observable.

I. Introduction

One of the most well-known manifestations of quantum mechanics must be the tunneling effect in the ammonia molecule, where the vibration–rotation energy levels anticipated for the rigid molecule are found to be doubled. It occurs due to the interaction between wave functions localized at the two distinct minima on the potential energy surface (PES) which interconvert via a planar D_{3h} transition state.[1,2] There has recently been renewed interest in the tunnel effect due to advances in spectroscopic techniques and the realization that tunneling splittings can provide detailed information about intermolecular forces from the insight they provide into the underlying PES. Van der Waals dimers have been particularly popular subjects for study, including $(NH_3)_2$,[3] $(H_2O)_2$,[4] and $(HF)_2$,[5,6] among others.[7] Hydrogen-bonded systems, especially water clusters, are especially interesting because of the unique importance of water,[7] and Pugliano and Saykally have recently presented results for $(H_2O)_3$ employing far-infrared vibration–rotation tunneling spectroscopy.[8] A detailed analysis of the latter system, based upon new theoretical calculations and the approach described in the present work, is given in an accompanying paper.[9] Inversion of detailed spectroscopic results to provide accurate empirical PES's is also being actively pursued by several groups.[10]

Here we predict the tunneling splittings for a variety of model cluster systems, some of which are bound by empirical potentials and others whose structures have been calculated *ab initio*. Information obtained by characterizing the relevant rearrangement pathways is used to map the multidimensional problem onto a simple one-dimensional model and, hence, to obtain estimates of the tunneling matrix elements between minima.

II. Reaction Path Characterizations

All the determinations of minima, transition states, and minimum energy reaction pathways were performed by eigenvector-following[11] (EF), and many of the mechanisms investigated in this paper have been reported in earlier works,[12–17] if only in terms of the transition states and the minima that they link. The particular EF algorithm has been described before;[18] the present calculations were conducted in Cartesian coordinates following Baker and Hehre[19]—some calculations of this sort for clusters bound by model potentials were recently reported.[20] In each case, analytic first and second derivatives of the energy were

® Abstract published in *Advance ACS Abstracts*, November 1, 1993.

(1) Dennison, D. M.; Hardy, J. D. *Phys. Rev.* **1932**, *39*, 938. Sheng, H.-S.; Barker, E. F.; Dennison, D. M. *Phys. Rev.* **1941**, *60*, 786.

(2) Bell, R. P. *The Tunnel Effect in Chemistry*; Chapman and Hall: New York, 1980. Dennison, D. M.; Uhlenbeck, G. E. *Phys. Rev.* **1932**, *41*, 313.

(3) Nelson, D. D.; Fraser, G. T.; Klemperer, W. *J. Chem. Phys.* **1987**, *83*, 6201. Nelson, D. D.; Klemperer, W.; Fraser, G. T.; Lovas, F. J.; Suenram, R. D. *J. Chem. Phys.* **1987**, *87*, 6364. Nelson, D. D.; Klemperer, W. *J. Chem. Phys.* **1987**, *87*, 139. Loeser, J. G.; Schuttenmaer, C. A.; Cohen, R. C.; Elrod, M. J.; Steyery, D. W.; Saykally, R. J.; Bumgarner, R. E.; Blake, G. A. *J. Chem. Phys.* **1992**, *97*, 4727.

(4) Odutola, J. A.; Hu, T. A.; Prinslow, D. A.; O'dell, S. E.; Dyke, T. R. *J. Chem. Phys.* **1988**, *88*, 5352. Fraser, G. T. *Int. Rev. Phys. Chem.* **1991**, *10*, 189. Dyke, T. R. *J. Chem. Phys.* **1977**, *66*, 492. Pugliano, N.; Saykally, R. J. *J. Chem. Phys.* **1992**, *96*, 1832.

(5) Dyke, T. R.; Howard, B. J.; Klemperer, W. *J. Phys. Chem.* **1972**, *56*, 2442.

(6) Bunker, P. R.; Carrington, T.; Gomez, P. C.; Marshall, M. D.; Kofranek, M.; Lischka, H.; Karpfen, A. *J. Chem. Phys.* **1989**, *91*, 5154. Jensen, P.; Bunker, P. R. *J. Chem. Phys.* **1990**, *93*, 6266. Bunker, P. R.; Jensen, P.; Karpfen, A.; Kofranek, M.; Lischka, H. *J. Chem. Phys.* **1990**, *22*, 7432. Althorpe, S. C.; Clary, D. C.; Bunker, P. R. *Chem. Phys. Lett.* **1991**, 345.

(7) Saykally, R. J.; Blake, G. A. *Science* **1993**, *259*, 1570.

(8) Pugliano, N.; Saykally, R. J. *Science* **1992**, *257*, 1937.

(9) Wales, D. J. *J. Am. Chem. Soc.*, preceding paper in this issue.

(10) Cohen, R. C.; Saykally, R. J. *Annu. Rev. Phys. Chem.* **1991**, *42*, 369. Hutson, J. M. *Annu. Rev. Phys. Chem.* **1990**, *41*, 123. Hutson, J. M. *J. Phys. Chem.* **1992**, *96*, 4237.

(11) Cerjan, C. J.; Miller, W. H. *J. Chem. Phys.* **1981**, *75*, 2800. Simmons, J.; Jørgenson, P.; Taylor, H.; Ozment, J. *J. Phys. Chem.* **1983**, *87*, 2745. O'Neal, D.; Taylor, H.; Simmons, J. *J. Phys. Chem.* **1984**, *88*, 1510. Banerjee, A.; Adams, N.; Simmons, J.; Shepard, R. *J. Phys. Chem.* **1985**, *89*, 52. Baker, J. *J. Comput. Chem.* **1986**, *7*, 385. Baker, J. *J. Comput. Chem.* **1987**, *8*, 563.

(12) Wales, D. J. *J. Chem. Phys.* **1989**, *91*, 7002. Wales, D. J. *Chem. Phys. Lett.* **1990**, *166*, 419. Davis, H. L. D.; Wales, D. J.; Berry, R. S. *J. Chem. Phys.* **1990**, *92*, 4308. Doye, J. P. K.; Wales, D. J. *J. Chem. Soc., Faraday Trans.* **1992**, *88*, 3295. Wales, D. J. *J. Am. Chem. Soc.* **1993**, *115*, 1557. Wales, D. J. *J. Am. Chem. Soc.* **1990**, *112*, 7908. Wales, D. J.; Waterworth, M. *J. Chem. Soc., Faraday Trans.* **1992**, *88*, 3409.

(13) Braier, P. A.; Berry, R. S.; Wales, D. J. *J. Chem. Phys.* **1990**, *93*, 8745.

(14) Rafac, R.; Schiffer, J. P.; Hangst, J. S.; Dubin, D. H. E.; Wales, D. J. *Proc. Natl. Acad. Sci. U.S.A.* **1991**, *88*, 483. Wales, D. J.; Lee, A. M. *Phys. Rev. A* **1993**, *47*, 380.

(15) Wales, D. J.; Bone, R. G. A. *J. Am. Chem. Soc.* **1992**, *114*, 5399.

(16) Wales, D. J.; Ohmine, I. *J. Chem. Phys.* **1993**, *98*, 7245 and 7257.

(17) Wales, D. J. *Mol. Phys.* **1991**, *74*, 1.

(18) Wales, D. J. *J. Chem. Soc., Faraday Trans.* **1990**, *86*, 3505; **1992**, *88*, 653.

(19) Baker, J.; Hehre, W. J. *J. Comput. Chem.* **1991**, *12*, 606.

(20) Wales, D. J. *J. Chem. Soc., Faraday Trans.* **1993**, *89*, 1305.

0002-7863/93/1515-11191$04.00/0

employed throughout, and a maximum step size criterion was used to scale the steps if needed.[20]

To calculate the minimum energy reaction pathways, the transition states were first perturbed by displacing the geometries in both directions along the reaction path according to the unique normal mode corresponding to the direction of negative curvature.[21] The required displacements are obtained by dividing the components of the normal mode vector by the square root of the appropriate atomic mass and then dividing by 50 to obtain a suitably small perturbation. The magnitude of the displacement is not usually critical, though one sensitive case is identified for $(H_2O)_3$ in the companion paper.[9] Having obtained the perturbed geometries, the pathway is followed by performing EF searches for minima. The smaller the EF steps are, the closer the optimization should be to the minimum energy reaction path;[22] however, high accuracy is not appropriate in the present context, and most of the calculations reported here used a maximum step size of 0.15 units (either bohr or angstrom, as appropriate).

Most of the reaction pathways are visualized using Mathematica[23] to plot nine configurations from the rearrangement. The first and last are always the two minima in question, and the middle one is the transition state. The remaining six frames were selected at regular spacings along the two downhill paths, three on each side. Where possible the clusters are triangulated to give a better three-dimensional impression of the change in shape. A suitably scaled set of displacement vectors corresponding to the normal mode with the unique imaginary frequency is also superimposed upon the transition state in most cases.

III. Estimating the Tunneling Matrix Elements

One object of the present work is to provide a rapid estimate of the magnitude of possible tunneling effects and the associated splitting patterns for various model clusters. More accurate calculations of tunneling states have certainly been performed previously, using both semiclassical[2] and fully quantum mechanical approaches.[6] However, the number of degrees of freedom in some of the present cases makes the mapping of these problems onto the one-dimensional semiclassical model[2] or an *ab initio* method somewhat problematic. The present treatment can provide an estimate of the order of magnitude of the tunneling splitting for both symmetrical and asymmetrical barriers using information from the reaction path; hence we can draw some conclusions, albeit qualitative, about tunneling in the more complicated systems.

Since the splitting patterns are determined by symmetry, while the numerical values require further approximations, the former are likely to be more reliable than the latter. However, the Hückel-type treatment described below could be combined with more accurate calculations of the tunneling matrix elements, or the predicted splitting patterns could be fitted to experimental data to obtain these parameters. As the rectangular well model employed in the present work is rather crude, it would probably not be profitable to extend such fitting to the barrier heights and widths.

The discussions of the molecular symmetry group[24,25] in the following section require us to consider molecules where atoms of the same element are distinguished by labels. As some of the notation is also used in the present section, it is convenient to introduce it here. When discussing labeled atom species it is important to be specific about whether one is talking about geometries that are structurally distinct or geometries which only differ in terms of the labels carried by atoms of the same element. In this work the nomenclature of Bone *et al.* will be used: a "structure" refers to a particular geometry and a "version" refers to a structure with a particular labeling scheme.[26] Minima that are directly linked by a given rearrangement in a single step are said to be "adjacent".

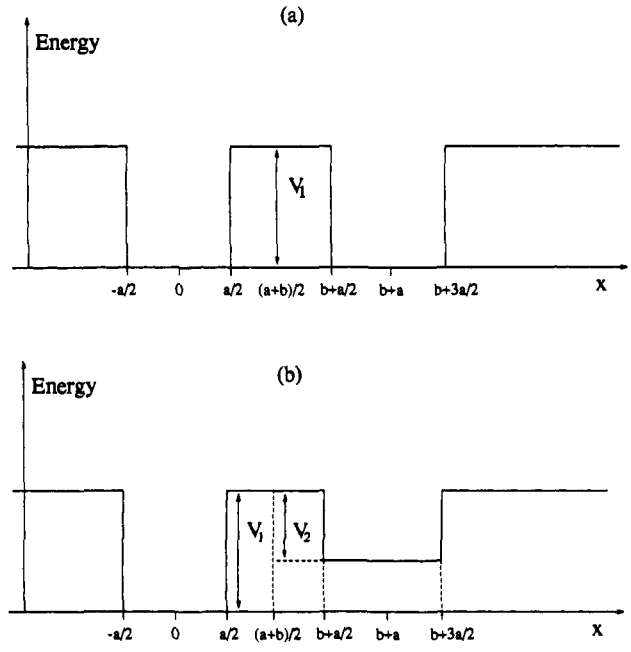

Figure 1. Model one-dimensional potentials considered in this work for the estimation of tunneling matrix elements: (a) equivalent structures, (b) different structures.

The approach adopted here is analogous to the linear combination of atomic orbitals (LCAO) method for the construction of molecular orbitals. If there are n distinguishable versions of a given structure, then there are n degenerate wave functions, each localized in one particular potential energy well, for any given vibration–rotation state of the molecule. In the simplest case, where rearrangements occur only between these n distinguishable versions, we may approximate the true wave function as a linear combination of localized wave functions (LCLW).[27] Applying the variational principle then leads to a set of secular equations, just as in standard molecular orbital theory. The eigenvalues of the secular determinant give the tunneling energy levels, and the corresponding eigenvectors must transform according to irreducible representations of the effective molecular symmetry group (section IV). Hence, to set up the secular determinant, we require the Hamiltonian and overlap matrix elements of the localized functions.

Degenerate rearrangements are those which link minima that have the same geometry if atoms of the same element are not distinguished.[28] In the simplest, but important, case we consider one type of degenerate rearrangement mechanism which links n versions of the same structure. Here, all the diagonal matrix elements of $\mathcal{H}$ are the same, and the off-diagonal elements of $\mathcal{H}$ are denoted by β, the tunneling matrix element, if the corresponding minima are directly linked by the rearrangement (adjacent), and are set to zero otherwise. Analogous assumptions are made for the overlap matrix. Since the localized basis functions decay exponentially in classically forbidden regions, this Hückel-type approximation can be quite good.

The problem of finding which minima are directly connected is addressed in the next section. To estimate β, we consider the one-dimensional model shown in Figure 1a. The textbook solution of the single-well Schrödinger equation is[29]

(21) Murrell, J. N.; Laidler, K. J. *Trans. Faraday Soc.* **1968**, *64*, 317.
(22) Fukui, K. *J. Phys. Chem.* **1970**, *74*, 4162. Fukui, K. *Acc. Chem. Res.* **1981**, *14*, 363. Miller, W. H.; Handy, N. C.; Adams, J. E. *J. Chem. Phys.* **1980**, *72*, 99. Pechukas, P. *J. Chem. Phys.* **1976**, *64*, 1516. Banerjee, A.; Adams, N. P. *Int. J. Quantum Chem.* **1992**, *43*, 855.
(23) Mathematica 2.0; Wolfram Research Inc., Champaign, IL, 1989.
(24) Longuet-Higgins, H. C. *Mol. Phys.* **1963**, *6*, 445.
(25) Bunker, P. R. *Molecular Symmetry and Spectroscopy*; Academic Press: New York, 1979.

$$\psi(x_1) = \begin{cases} -\infty < x_1 < -a/2, & C_1 \exp(x_1\sqrt{2m(V_1 - E)}/\hbar), \\ -a/2 < x_1 < a/2, & B_1 \cos(x_1\sqrt{2mE}/\hbar - n\pi/2), \\ a/2 < x_1 < \infty, & (-1)^n C_1 \exp(-x_1\sqrt{2m(V_1 - E)}/\hbar), \end{cases} \quad (1)$$

where $x_1 \equiv x$ in this case, a is the width of the well, B_1 and C_1 are defined by normalization and continuity conditions, and the energy, E, is determined by solution of

$$\sqrt{V_1 - E} = \sqrt{E}\tan(a\sqrt{2mE}/2\hbar + n\pi/2). \quad (2)$$

There is always at least one bound state.[29] To estimate β, we now consider the second well, for which the wave functions, $\psi(x_2)$, in the absence of the first well are the same as above, but with $x_2 = x - (a + b)$. Hence

$$\beta = \langle\psi(x_1)|\mathcal{H}|\psi(x_2)\rangle$$

$$\approx C_1^2 \int_{a/2}^{b+a/2} e^{-x\sqrt{2m(V_1 - E)}/\hbar}\left(-\frac{\hbar^2}{2m}\frac{d^2}{dx^2} + V_1\right)e^{(x-a-b)\sqrt{2m(V_1 - E)}/\hbar}\,dx$$

$$= C_1^2 Eb \exp(-(a + b)\sqrt{2m(V_1 - E)}/\hbar), \quad (3)$$

where $\mathcal{H}$ is the true Hamiltonian which includes both wells, contributions from outside the region between the two wells have been neglected, and the normalization constants are the same by symmetry if we arrange for the localized functions to be combined in phase. This approximation gives $\beta = ES$ where S is the overlap integral $\langle\psi(x_1)|\psi(x_2)\rangle$. However, despite this result, $\psi(x_2)$ and $\psi(x_1)$ are not eigenfunctions of $\mathcal{H}$ when both wells are present;[30] if they were, then no tunneling splittings would occur. Similarly, the diagonal elements of $\mathcal{H}$ are not equal to the unperturbed energy E because of the presence of the second well.

The secular problem which determines the tunneling states is defined by $|H - ES| = 0$, where S and H are the usual overlap and Hamiltonian matrices, respectively. The required matrix elements were calculated from analytic expressions without neglecting any contributions from particular regions. For systems where the tunneling is found to be large the wave functions may decay slowly enough in the classically forbidden regions for the approximation inherent in eq 3 to be poor. In one case (the very facile "flipping" mechanism of water trimer, discussed elsewhere[9]), the overlap integrals calculated between the "localized" functions of the neighboring wells are so close to unity that the overlap matrix, S, has a negative eigenvalue. Here the barrier is so low that the corresponding motion is more like a perturbed translation than a large amplitude vibration, and the LCLW secular problem is not well-defined.

In fact, it is more convenient to discuss the results with reference to the model secular problem in which the diagonal elements of H are set to zero and the off-diagonal overlap integrals are neglected. The roots of the secular determinant can then usually be written straightforwardly in terms of β, and various helpful analogies with simple Hückel theory can be exploited. If we denote the levels of this idealized problem by λ', and those obtained without neglecting off-diagonal overlap and the diagonal elements of H by λ, then there is usually an essentially exact linear mapping $\lambda = c + d\lambda'$ between the two. The results are therefore summarized by giving the levels for the model problem in terms of β, along with the numerical value of $d \times \beta$, where d is the scaling factor in the above mapping. When the tunneling effect is calculated to be negligible, the value of β itself is given. If more than one mechanism is feasible, then experiment can tell which it is that leads to the biggest splittings even if we only know the splitting pattern in terms of β parameters.

In three cases (for Morse clusters M_6 with M = Ne), the mapping is distinctly nonlinear, and the effective β values quoted for $d \times \beta$ use the best-fit value of d. When two types of rearrangement are involved, the scaling factor for the tunneling levels when both mechanisms are considered together may be different from when they are considered separately, and this information will also be given.

To evaluate β, we need to know C_1^2, E, a, b, and m, all of which were obtained by mapping the multidimensional reaction pathway onto the above double-well potential in an intuitive fashion. Once the barrier and mass, V_1 and m, are known, the energy levels can be found by numerical solution of eq 2, and once E has been calculated, the normalization constants may be determined numerically using continuity conditions. Both tasks were performed using Mathematica;[23] high-precision arithmetic was required in some cases where β is very small. Although such cases will not be of experimental interest, the numbers are needed to tell us this. The lowest permitted eigenvalue was sought by starting Newton's root-finding method from a number of different guesses for E in the range 10^{-4}–10^{-16} hartree.[31] The lowest solution was generally found several times; given the other approximations, it is probably not crucial to locate the smallest eigenvalue, although the present procedure should usually do so. For want of any better information the barrier width b was simply set equal to the width of the potential wells, a, leaving just two parameters to be determined.

At this point it is convenient to introduce several properties of a reaction path which are helpful in discussing the above parameters. The path length $S = \int ds$ is the integrated arc length in $3N$-dimensional nuclear configuration space, where N is the number of atoms. S was calculated as a sum over the eigenvector-following steps:

$$S = \sum_{\text{steps}} \sqrt{\sum_i \Delta Q_i^2} \quad (4)$$

where ΔQ_i is the step for nuclear Cartesian coordinate Q_i (not mass-weighted) and the outer sum is over all the eigenvector-following steps. The discretization of the path does not lead to significant errors in S for the present purposes. The moment ratio of displacement, γ, is defined as[32]

$$\gamma = \frac{N\sum_i [Q_i(s) - Q_i(t)]^4}{(\sum_i [Q_i(s) - Q_i(t)]^2)^2} \quad (5)$$

where $Q_i(s)$ is the value of the nuclear Cartesian coordinate Q_i for minimum s, etc. If only a single atom moves (localized process), then $\gamma = N$, while if all atoms move through the same distance (cooperative process), then $\gamma = 1$; hence, γ provides a measure of how cooperative a rearrangement is. As the minimum energy pathways are calculated by projecting out overall translation and rotation at each step,[20] γ is simply evaluated using the relative positions of the two minima at the endpoints. (These pathways are not strictly equivalent to the results for steepest descent in mass-weighted coordinates but should be close enough for the present purposes.) The third parameter is the distance between minima in nuclear configuration space[33]

(26) Bone, R. G. A.; Rowlands, T. W.; Handy, N. C.; Stone, A. J. *Mol. Phys.* **1991**, *72*, 33.
(27) Bone, R. G. A. Ph.D. Thesis, Cambridge University, 1992.
(28) Leone, R. E.; Schleyer, P. v. R. *Angew. Chem., Int. Ed. Engl.* **1970**, *9*, 860.
(29) Johnson, C. S.; Pederson, L. G. *Problems and Solutions in Quantum Chemistry and Physics*; Dover: New York, 1986.
(30) Berry, R. S. *Rev. Mod. Phys.* **1960**, *32*, 447.
(31) The hartree and bohr radius, a_0, are the atomic units of energy and length, respectively, where 1 hartree = 4.359 748 × 10^{-18} J and a_0 = 5.291 772 × 10^{-11} m.
(32) Stillinger, F. H.; Weber, T. A. *Phys. Rev. A* **1983**, *28*, 2408.
(33) Tanaka, H.; Ohmine, I. *J. Chem. Phys.* **1989**, *91*, 6318. Ohmine, I.; Tanaka, H. *J. Chem. Phys.* **1990**, *93*, 8183.

$$D = \sqrt{\sum_i (Q_i(s) - Q_i(t))^2} \quad (6)$$

By definition $D \leq S$, and in the present work we take $D = 2a$. In choosing a value for the mass, m, we must allow for the fact that some of the system may be relatively unaffected by the rearrangement. This was achieved by defining

$$\gamma_m = \frac{N\sum_i m_i[Q_i(s) - Q_i(t)]^2}{\gamma\sum_i [Q_i(s) - Q_i(t)]^2} \quad (7)$$

If all the atoms move through the same distance, then γ_m is the total molecular mass, but if only one atom moves, then γ_m is the mass of that atom. In the present calculations we therefore take $m = \gamma_m$; an alternative possibility is considered in the Appendix.

Various assumptions are required to map the calculated reaction pathway onto the model one-dimensional problem, and we clearly cannot expect to produce better than an order of magnitude estimate for β with this approach. This in itself may be a useful guide to the most promising systems for further study, both by experiment and perhaps by more accurate calculations.[2,6] Furthermore, the division of splittings into "small", "medium", and "large", which is the most realistic ambition of the numerical calculations, may also be helpful, as for the water trimer.[9] As mentioned above, the symmetry-determined splitting patterns will probably be more reliable than the numerical values. The barriers used were not corrected for zero-point effects, as these should be included in the model problem by solving the appropriate Schrödinger equation.

To generalize this LCLW-type approach to systems with more than one sort of minimum should not be difficult. In this case we would need to calculate relative values of the diagonal elements of $\mathcal{H}$ for all the different local minima, along with off-diagonal elements for nondegenerate rearrangements between different structures. The off-diagonal elements may be estimated within the current framework by considering the model problem shown in Figure 1b. The solutions to eqs 1 and 2 for the two different wells are distinguished by the subscripts 1 and 2, and

$$\begin{aligned}\beta_{12} &= \langle\psi(x_1)|\mathcal{H}|\psi(x_2)\rangle \\ &= \tfrac{1}{2}(E_1 + E_2)\langle\psi(x_1)|\psi(x_2)\rangle - \\ &\quad \tfrac{1}{2}V_1\int_{-a/2}^{a/2}\psi(x_1)\psi(x_2)\,dx - \tfrac{1}{2}V_2\int_{b+a/2}^{b+3a/2}\psi(x_1)\psi(x_2)\,dx \\ &\approx \tfrac{1}{2}(E_1 + E_2)\langle\psi(x_1)|\psi(x_2)\rangle_{\text{barrier region}} \\ &= \frac{C_1C_2(E_1 + E_2)}{k_2 - k_1}e^{-a(k_1+k_2)}\sinh a(k_1 - k_2)/2 \end{aligned} \quad (8)$$

where $k_i = \sqrt{2m(V_1 - E_i)}/\hbar$, E_i are the lowest energy eigenvalues for the isolated wells (referred to a common energy zero), and the normalization constants may now be different. Note that in the limit $V_1 \to V_2$ we recover $\beta_{12} \to \beta$, while the factor $1/(k_2 - k_1)$ means that tunneling effects caused by the interaction of different structures will generally be smaller than for degenerate rearrangements, in agreement with previous work.[2] To estimate β_{12}, we therefore require the same reaction path data as before along with numerical solutions of the two isolated well problems. Two examples of this kind of calculation are reported in section V; as before, the actual values of β_{12} quoted were calculated from an analytic formula which does not neglect the contributions from any regions. The problem of setting up the corresponding secular problem using the LCLW approach has not yet been tackled.

IV. The Effective Molecular Symmetry Group

For molecules which undergo rearrangements on some given experimental time scale, the appropriate group in which to classify the energy levels is the effective molecular symmetry (MS) group introduced by Longuet-Higgins[24] and developed by Bunker.[25] To exploit this formalism, we must distinguish identical nuclei by means of labels. The operations of the MS group then consist of permutations, P, of identical nuclei amongst themselves, and permutation–inversions, P^*, where a permutation is combined with the inversion, E^*, of all particle coordinates through the origin of a space-fixed axis system. (E denotes the identity operation.) The complete nuclear permutation–inversion (CNPI) group contains all such operations, which all commute with the full molecular Hamiltonian.[24] However, to achieve some of these permutation–inversions may require bond-breaking or other processes that are effectively impossible under experimental conditions. This leads us to distinguish "feasible" operations which correspond to permutation–inversions that can actually occur. Even for an essentially rigid molecule, with no energetically feasible rearrangements available, some permutation–inversions are still possible. These form a subgroup of the CNPI group which is isomorphic to the rigid molecule point group.[25,34] The result of such operations is, at most, to reorient the original geometry, and hence they will be referred to as "barrierless" operations in this paper. The MS group contains all the permutation–inversions that are considered to be feasible for a given labeled version of the structure under the prevailing conditions, which may include operations corresponding to different rearrangement mechanisms.

To illustrate these ideas, consider the question of how many potential wells there are corresponding to a particular structure on a given potential energy surface (PES). The total number of permutation–inversion operations is $2 \times N_1! \times N_2! \times \ldots$, where there are N_i atoms of element i in the given structure. This is also the order of the CNPI group, h_{CNPI}. However, some of these labeling schemes correspond to the same versions and differ only in orientation, i.e. by barrierless operations. Since there are h_{PG}^{M} such operations, where h_{PG}^{M} is the order of the point group corresponding to the structure M, the number of minima is $h_{\text{CNPI}}/h_{\text{PG}}^{\text{M}}$, as is well-known.[35] This information is useful in applications where the global nature of the PES must be considered explicitly, for example, in the calculation of fractional residence times for different structures[36] or in the estimation of thermodynamic properties by summation of the phase space associated with different structures.[37] Similarly, the number of distinguishable transition states of a given structure that mediate a particular type of rearrangement for the same minimum is $h_{\text{CNPI}}/h_{\text{PG}}^{\text{TS}}$, and the connectivity at each vertex of the reaction network (or reaction graph) is therefore $2h_{\text{PG}}^{\text{M}}/h_{\text{PG}}^{\text{TS}}$. Bone *et al.*[26] have extended such considerations to prove that the number of versions linked by the operations of the MS group is $h_{\text{MS}}/h_{\text{PG}}$ for both minima and transition states.

We can apply these results to produce a concise derivation of the "reaction path degeneracy" recently reconsidered in terms of the CNPI group by Karas *et al.*[38] Reaction rates are often calculated from formulas that employ the ratio of transition state to reactant density of states, such as the standard RRKM expression.[39] These densities of states should contain the number of distinct versions of the given structure as a factor,[36] and so the result can be written as $h_{\text{PG}}^{\text{M}}/h_{\text{PG}}^{\text{TS}}$ times the ratio of the densities of states for one version of each structure. (A further factor of 2 is needed for degenerate rearrangements because half the minima then correspond notionally to products.[38])

To deduce the reaction graph, simple algorithms were employed which are inherent in the theory that has developed the connection

(34) Hougen, J. T. *J. Chem. Phys.* **1963**, *39*, 358; **1962**, *37*, 1433.
(35) Dalton, B. J. *Mol.* Phys. **1966**, *11*, 265.
(36) Amar, F. G.; Berry, R. S. *J. Chem. Phys.* **1986**, *85*, 5943.
(37) Wales, D. J. *Mol. Phys.* **1993**, *78*, 151.
(38) Karas, A. J.; Gilbert, R. G.; Collins, M. A. *Chem. Phys. Lett.* **1992**, *193*, 181.
(39) Forst, W. *Theory of Unimolecular Reactions*; Academic: New York, 1973.

between double cosets and molecular rearrangements.[40] The input to the program starts with the number of different atoms of each element and sufficient generator permutation–inversions to produce all the barrierless operations, denoted by b_i, for a particular reference labeling of the minimum in question. (Extension to problems with more than one kind of minimum would be possible along similar lines.) The complete group $\mathcal{G}_{PG}$, of dimension h_{PG}^{M}, has been generated when all the products b_ib_j for b_i, $b_j \in \mathcal{G}_{PG}$ are themselves members of $\mathcal{G}_{PG}$. At this stage we also know h_{CNPI} and the number of distinct versions of the minimum. Note that $\mathcal{G}_{PG}$ is isomorphic to the rigid molecule point group but consists of permutation–inversion operations.

The generators for the feasible rearrangements are then read, together with the appropriate β elements. Let the generator for the ith type of feasible rearrangement of the reference minimum be g_i. As Bone has emphasized,[41] the operations in the coset $g_i\mathcal{G}_{PG}$ all link the reference minimum to the same version in a single step. For the rearrangements illustrated, g_i is chosen, wherever possible, to be a self-inverse operation of the appropriate transition state. However, for asymmetrical degenerate rearrangements, where the forward and reverse paths from the transition state are not equivalent, no such generator exists.[42] A minimal set of operations linking the reference minimum to all the different adjacent versions was determined by considering the products $b_j^{-1}g_ib_j$. If an operation linking the reference version to some adjacent version is M_j, then the barrierless operations of that adjacent version are given by the set of products $M_jb_kM_j^{-1}$. Hence, duplicate versions in the set $b_j^{-1}g_ib_j$ are easily identified because we can test whether they are related by barrierless operations. In the present context the connectivity of the reaction graph is taken to mean the number of distinct versions adjacent to the reference: multiple connections on the PES between adjacent versions are counted only once. Connectivities greater than 2 are often associated with rearrangements whose initial displacements correspond to degenerate normal coordinates.[26]

It may be helpful to compare some of the above formulas with a more familiar similarity transformation. For example, if the matrix corresponding to a given rotation about axis a is **A**, then the corresponding rotation about an axis b is given by $\mathbf{B} = \mathbf{C}^{-1}\mathbf{AC}$, where the rotation represented by **C** maps axis b onto axis a. Hence we consider the products $b_j^{-1}g_ib_j$ to cover cases where the same mechanism may be applied to the reference version in more than one way. For example, in the DSD process for $B_8H_8^{2-}$ (Figure 4) any of four equivalent edges may be broken initially. The formula for the barrierless operations of an adjacent version is directly analogous to the example of rotations about different axes given above.

The whole reaction graph was then calculated by considering a minimal set of MS group operations, M_i, which transform the reference minimum into each version precisely once. In other words, we choose a set of h_{MS}/h_{PG}^{M} operations which is in one-to-one correspondence with the versions that are linked by the operations of the MS group.

It then remains to test which members of this set are adjacent to each other. For each mechanism we have already determined the minimal set of operations which link the reference minimum to all its adjacent versions. The corresponding operations for any other version which is itself obtained by operation M_i from the reference minimum have the form $M_i(b_j^{-1}g_kb_j)M_i^{-1}$. We must also allow for barrierless operations to occur before or after such rearrangements, when comparing the results with the other versions in the set.

It is not claimed that the above procedure is an any way original or efficient, merely that it is correct, and was convenient to program. In fact, some of the procedures employed will rapidly become unmanageable for larger MS groups, but they were quite satisfactory for all the examples in this paper, except $B_8H_8^{2-}$, for which the MS group was already known.

Systems with more than one kind of rearrangement were treated by assuming that the degrees of freedom corresponding to different mechanisms are independent. Hence the diagonal Hamiltonian matrix elements resulting from solving the different one-dimensional problems were simply added.[43] In cases where adjacent versions are linked by more than one mechanism (or, indeed, by the same sort of mechanism via distinct versions of the same transition state), the corresponding off-diagonal element of $\mathcal{H}$ was simply set equal to the largest appropriate value of β; the overlap matrix was dealt with similarly. The class structure of the MS group was also calculated in order to deduce the allowed electric dipole transitions within a given manifold of tunneling states. This program and the Mathematica[23] scripts which evaluate β are available upon request from the author.[44]

V. Results

A detailed analysis of the water trimer is provided in an accompanying paper.[9] The new results presented in the present report may be divided into calculations which employ either *ab initio* or empirical potentials. *Ab initio* geometry optimizations and reaction pathway calculations were performed for $(HF)_2$, $C_5H_5^+$, and $B_8H_8^{2-}$. For $(HF)_2$ much more accurate calculations and experimental results for the tunneling splittings are available[6] with which to compare the present approach, while for $C_5H_5^+$ and $B_8H_8^{2-}$ the MS groups have been analyzed previously[15] and provide a test of the program that sets up the secular determinant. The empirical potentials employed are Morse[45] and Lennard-Jones[46] and a more complicated potential which includes atom–atom Lennard-Jones terms and the induction energy for benzene–Ar_1 and benzene–Ar_2. The Morse and Lennard-Jones clusters considered are M_6, $[LJ]_3$, and $[LJ]_4$, in the commonly used notation where M stands for Morse (not metal), etc. Note that nuclear spin statistics have not been considered, and these would be needed to predict the relative intensities of the spectral transitions.[24,47]

$(HF)_2$. For this species it has recently been possible to obtain tunneling splittings from detailed theoretical analyses which are in good agreement with experiment.[6] The values depend upon the vibrational state of the complex and typically lie between about 0.2 and 0.7 cm^{-1}. In this case the complex is sufficiently small for double-ζ[48] plus polarization basis sets (DZP) and the second-order Møller–Plesset correlation correction[49] to be employed in the reaction path calculations. The polarization functions consisted of a single set of p orbitals on each hydrogen (exponent 1.0) and a single set of six d orbitals on each fluorine (exponent 1.2) to give 42 basis functions in total. The geometry of the C_{2h} transition state, energy –200.518 323 hartrees, for the trans-tunneling process in question is shown in Figure 2; the parameters are in reasonable agreement with more accurate calculations.[6] The C_s minimum has energy –200.103 118 hartrees, giving a barrier of 0.001 312 hartree or 288 cm^{-1} (3.44 kJ mol^{-1}). The frequencies, in cm^{-1}, are, for the minimum, 4182,

(40) Klemperer, W. G. *J. Chem. Phys.* **1972**, *56*, 5478; *J. Am. Chem. Soc.* **1972**, *94*, 6940 and 8360; **1973**, *95*, 380 and 2105. Muetterties, E. L. *J. Am. Chem. Soc.* **1969**, *91*, 4115. Nourse, J. G. *J. Am. Chem. Soc.* **1976**, *99*, 2063. Brocas, J. *J. Am. Chem. Soc.* **1986**, *108*, 1135. Balasubramanian, K. *Chem. Rev.* **1985**, *85*, 599. Hässelbarth, W.; Ruch, E. *Theor. Chim. Acta* **1973**, *29*, 259. Brocas, J.; Fastenakel, D. *Mol. Phys.* **1975**, *30*, 193. Dalton, B. J.; Brocas, J.; Fastenakel, D. *Mol. Phys.* **1976**, *31*, 1887.

(41) Bone, R. G. A. *Chem. Phys. Lett.* **1992**, *193*, 557.

(42) Nourse, J. G. *J. Am. Chem. Soc.* **1980**, *102*, 4883.

(43) One might argue that the same should be done when a given mechanism links the reference minimum to more than one version. This has not been tested here, but it is unlikely to make a significant difference in the order of magnitude of the predicted splittings.

(44) Send requests to dw34@cus.cam.ac.uk.

(45) Morse, P. M. *Phys. Rev.* **1929**, *34*, 57.

(46) Jones, J. E.; Ingham, A. E. *Proc. R. Soc. London, A* **1925**, *107*, 636.

(47) Balasubramanian, K.; Dyke, T. R. *J. Phys. Chem.* **1984**, *88*, 4688 and references therein.

(48) Dunning, T. H. *J. Chem. Phys.* **1970**, *53*, 2823. Huzinaga, S. *J. Chem. Phys.* **1965**, *42*, 1293.

(49) Møller, C.; Plesset, M. S. *Phys. Rev.* **1934**, *46*, 618.

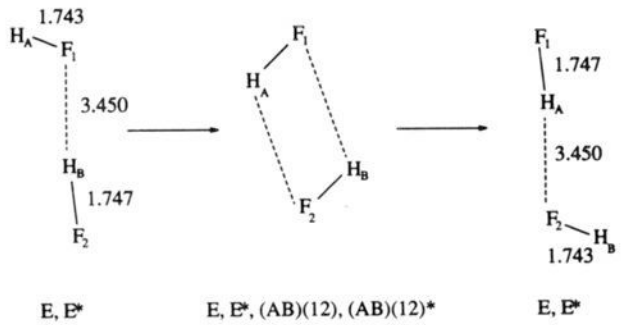

Figure 2. Trans-tunneling rearrangement of $(HF)_2$. The distances, in bohrs, were calculated at the DZP/MP2 level of theory, and the barrierless operations of each stationary point are also indicated.

4118, 593, 482, 221, and 168, and for the transition state, 4167, 4147, 618, 449, 175, and 176*i*, so the barrier corrected for zero-point effects (neglecting the imaginary frequency) is about 184 cm^{-1}.

The calculated reaction path consists of 32 eigenvector-following steps in this case, from which we find $S = 3.937\ a_0$, $\gamma = 1.81$, $\gamma_m = 4.17$ amu, $D = 3.246\ a_0$, and $\beta = -0.014\ cm^{-1}$. Note that this rearrangement is relatively delocalized in character, as indicated by the value of γ. In this case the generator is (AB)-(12) (in cycle notation, where A replaces B and 1 replaces 2) for the labeling scheme in Figure 2 and the MS group is isomorphic to C_{2v}. $h_{CNPI} = 8$, $h_{MS} = 4$, and there are 4 distinct minima, connected in two isolated pairs, giving doublet splittings of the rigid molecule energy levels. Electric dipole transitions between partner levels of a given doublet are not allowed. The tunneling splitting is $2|\beta| = 0.028\ cm^{-1}$, which is about 1 order of magnitude smaller than the experimental value.[16] Using the lower zero-point-corrected barrier in this case gives $\beta = 0.034\ cm^{-1}$. If the total mass of the cluster is used instead of γ_m, then $\beta = 3.1 \times 10^{-11}\ cm^{-1}$, and employing S instead of D for the total path length gives $\beta = 0.000\ 73\ cm^{-1}$. Although the splitting obtained with the zero-point-corrected barrier is somewhat closer to reality, none of these alternative calculations of β provides a compelling reason to change the framework previously described.

Systematic variation of one of the three parameters D, γ_m, or the barrier height, keeping the other two fixed, shows that β decreases with γ_m but has a maximum value for both D and the barrier height.

$C_5H_5^+$. The archetypal square–diamond, diamond–square (SDDS) rearrangement of square-based pyramidal $C_5H_5^+$ via a C_{2v} symmetry transition state was recently analyzed in detail including geometry optimizations at the DZP/MP2 level.[15] For the present purposes the pathway was calculated using minimal STO-3G basis sets (Figure 3), but the barrier employed in the calculation of β was the DZP/MP2 value (126.4 kJ mol^{-1}). The results (for a path consisting of 31 steps) are $S = 5.342\ a_0$, $\gamma = 2.97$, $\gamma_m = 9.64$ amu, $D = 4.633\ a_0$, and $\beta = 8.7 \times 10^{-45}\ cm^{-1}$. In this case it is the relatively large barrier to rearrangement which results in the very small tunneling splitting, and the effect clearly lies well beyond the limits of experimental resolution.

Using the same labeling scheme as in the previous analysis[15] (Figure 3), the required generator is (de)(bc); since the CH units move as well-defined entities in this case, there is no need to specify the permutations for the hydrogen atoms as well. $h_{CNPI} = 28\ 800$ and $h_{MS} = 240$, which is the largest MS group that is possible without breaking C–H terminal bonds. Hence the minima occur in 120 separate sets or "domains"[50] within which each minimum is connected to four others and the tunneling states and energies (with degeneracies in parentheses) are

$\Gamma_1^+(1)$	$\Gamma_4^-(4)$	$\Gamma_5^+(5)$	$\Gamma_6^-(5)$	$\Gamma_3^+(4)$	$\Gamma_6^+(5)$	$\Gamma_7^-(6)$
4β	3β	2β	0	$-\beta$	-2β	-2β

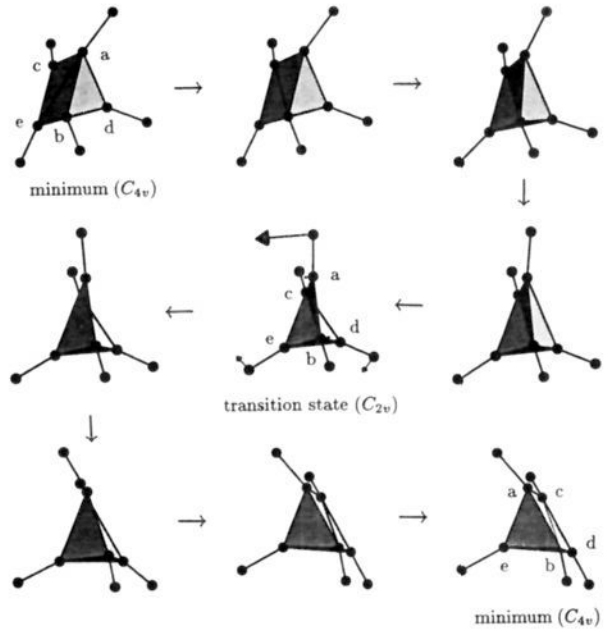

Figure 3. SDDS rearrangement of $C_5H_5^+$ calculated *ab initio* using minimal STO-3G basis sets.

using the notation of Hamermesh[51] for the irreducible representations. In the previous analysis it was not possible to distinguish between Γ_5^+ and Γ_6^+. However, as the program which sets up the secular matrix also calculates the characters of the tunneling states, the above pattern can now be confirmed. The only allowed electric dipole transition within this manifold is between Γ_6^+ and Γ_6^- of energy 2β. (If the MS group contains the inversion E*, then the irreducible representations can be classified as odd or even under this operation and the electric dipole selection rule is $\Gamma^+ \leftrightarrow \Gamma^-$.) The accidental degeneracy at -2β is typical of Hückel-type analyses,[52] and some other aspects of simple Hückel theory carry over also. For example, because the splitting pattern is not symmetrical about the energy origin, we know that the reaction graph must contain at least one odd-membered ring. This may be deduced from the analogue of the Coulson–Rushbrooke pairing principle[53] for alternant Hückel systems: for an alternant reaction graph (one containing no odd-membered rings), the splitting pattern must obey a mirror relation with respect to the energy origin. The eigenvalue of 4β simply reflects the connectivity of the reaction graph—it corresponds to the totally in-phase linear combination of localized functions.

$B_8H_8^{2-}$. The archetypal diamond–square–diamond (DSD) rearrangement in $B_8H_8^{2-}$ was also investigated[15] in the same study as $C_5H_5^+$. For the present purposes the reaction pathway was calculated using minimal STO-3G basis sets (Figure 4), and the barrier used in the calculation of β was the DZP/MP2 value of 28.1 kJ mol^{-1}, giving the following results: $S = 4.750\ a_0$, $\gamma = 2.07$, $\gamma_m = 30.26$ amu, $D = 4.172\ a_0$, $\beta = 3.0 \times 10^{-34}\ cm^{-1}$. Note that this rearrangement is more delocalized than the SDDS processes for $C_5H_5^+$, according to the values of γ. This time the path contained 27 steps, and β is small due to the combination of a relatively high barrier and a relatively large value of γ_m. For the labeling scheme in Figure 4 the generator is (ab)(cd)(eh)*, where, as for $C_5H_5^+$, the corresponding permutations of the hydrogen atoms are omitted. $h_{CNPI} = 2 \times (8!)^2$ and $h_{MS} = 80\ 640$, which is the largest MS group that is possible without breaking B–H terminal bonds. There are 10 080 distinct minima in each

(50) Watson, J. K. G. *Can. J. Phys.* **1965**, *43*, 1997.
(51) Hamermesh, M. *Group Theory and its Application to Physical Problems*; Dover: New York, 1989; p 188.
(52) Hall, G. G. *Mol. Phys.* **1977**, *83*, 551.
(53) Coulson, C. A.; Rushbrooke, S. *Proc. Cambridge Philos. Soc.* **1940**, *36*, 193.

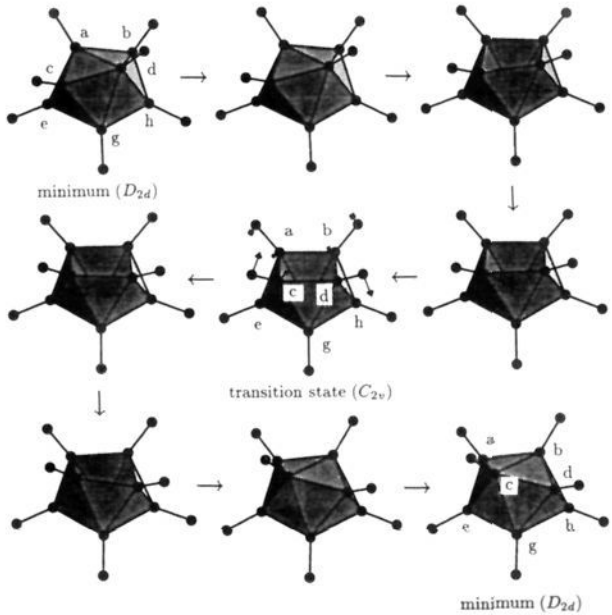

Figure 4. DSD rearrangement of $B_8H_8^{2-}$ calculated *ab initio* using minimal STO-3G basis sets. Vertex f is always hidden.

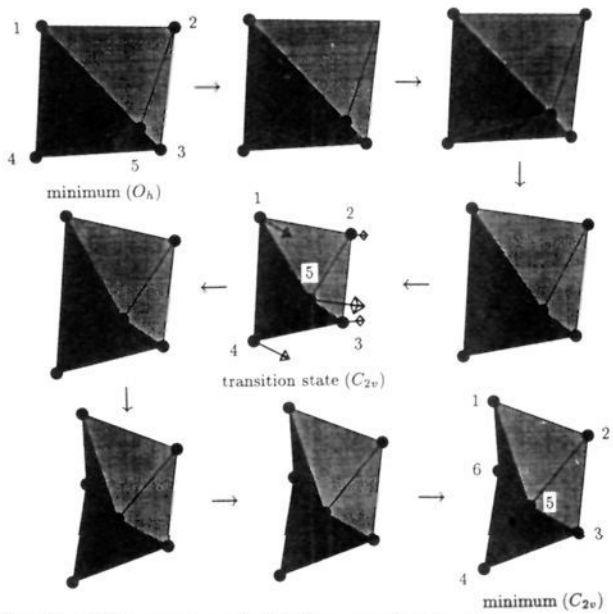

Figure 5. DSD rearrangement of M_6 from an octahedron to an incomplete pentagonal bipyramid calculated at $\rho_0 = 6$.

of the 40 320 unconnected domains, so in this case no attempt was made to construct or diagonalize the secular matrix. However, the largest eigenvalue must be 4β because the reaction graph is 4-connected.

M_6. The properties of the M_6 Morse cluster were studied as a function of the range of the potential by Braier *et al.*,[13] and the evolution of the MS group as the topology of the PES changes has also been considered.[13,54] The Morse potential may be scaled so that there is one free parameter, ρ_0, which governs the range of this isotropic pair potential.[13] Small values of ρ_0 correspond to a long-range potential and large values to a short-range potential; when $\rho_0 \approx 6$, the curvature at the equilibrium pair separation matches that of the Lennard-Jones potential. The global minimum for $1 < \rho_0 \leq 6$, the range considered here, is the regular octahedron. For $\rho_0 > 4.1$ there is one higher energy minimum, described as an incomplete pentagonal bipyramid[13] (IPB). The lowest energy rearrangement of the octahedron in this case is a simple DSD process[13] linking it to the IPB (Figure 5). For each IPB there are four possible DSD degenerate rearrangements with distorted capped square-based pyramidal (CSBP) transition states (Figure 6a). If one such process is followed by a rearrangement back to an octahedron, then an overall permutation–inversion of that structure may be effected. To estimate tunneling splittings, we need to choose values for the units of length and energy; here we calculate β using the well depth and equilibrium pair separation appropriate to Ar and Ne,[13] which are known from the properties of the corresponding diatomics.[55] The actual values of ρ_0 tabulated for Ar and Ne are 5.72 and 2.05, and so these example calculations[56] for $\rho_0 = 6$ are really more appropriate for Ar than Ne. Of course, for both the Morse and Lennard-Jones potentials all the classically defined quantities S, D, γ, γ_m, and the barrier height scale in an obvious way between Ar and Ne.

For the octahedron to IPB rearrangement (Figure 5), the reaction path consisted of 23 steps and the barriers are 0.000 26/0.000 12 and 0.000 049/0.000 022 hartree, for Ar and Ne, respectively. Using the asymmetric model problem, $S = 0.903$ a_0, $\gamma = 1.58$, $\gamma_m = 151.5$ amu, $D = 0.729$ a_0, and $\beta = 0.54$ cm^{-1} for Ar and $S = 0.415$ a_0, $\gamma = 1.58$, $\gamma_m = 75.75$ amu, $D = 0.336$ a_0, and $\beta = 8.5$ cm^{-1} for Ne. For the degenerate rearrangement of the IPB via a CSBP (Figure 6a), the path has 21 steps and the barrier is 0.000 29/0.000 055 hartree for Ar/Ne. Hence, $S = 1.325$ a_0, $\gamma = 1.32$, $\gamma_m = 181.9$ amu, $D = 1.087$ a_0, and $\beta = -0.000\ 78$ cm^{-1} for Ar and $S = 0.610$ a_0, $\gamma = 1.32$, $\gamma_m = 90.93$ amu, $D = 0.501$ a_0, and $\beta = 5.3$ cm^{-1} for Ne. For the somewhat higher energy degenerate rearrangement of the IPB via an edge-bridged trigonal bipyramid (Figure 6b), the path has 31 steps and the barrier is 0.000 39/0.000 074 hartree for Ar/Ne. Hence, $S = 1.961$ a_0, $\gamma = 1.40$, $\gamma_m = 172.1$ amu, $D = 1.510$ a_0, and $\beta = -7.8 \times 10^{-6}$ cm^{-1} for Ar and $S = 0.903$ a_0, $\gamma = 1.40$, $\gamma_m = 86.03$ amu, $D = 0.695$ a_0, and $\beta = 2.5$ cm^{-1} for Ne. Note that these mechanisms are all essentially delocalized. One may also treat the whole octahedron to octahedron path as a single step via either of the degenerate IPB rearrangements. Guessing the appropriate parameters from the above data gives $\beta = -2.6 \times 10^{-10}/0.43$ cm^{-1} for Ar/Ne using the CSBP path and $\beta = 1.5 \times 10^{-11}/0.13$ cm^{-1} for Ar/Ne using the edge-bridging path.

We may also treat the secular problem without explicitly including the IPB minimum by considering the octahedron interconversions as single steps with effective values of β. The generator for the degenerate rearrangement of the IPB shown in Figure 6a is (12)(53)*, and this is also a suitable self-inverse generator to describe the overall transformation from the octahedron in Figure 5 to the octahedron that results if a final DSD process occurs for the IPB at the bottom right corner of Figure 6a. In previous work[13] this permutation was represented as (12)(365), but the self-inverse generator is preferred here. The connectivity of the reaction graph for the generator (12)(53)* is 8, $h_{CNPI} = 1440 = h_{MS}$, in agreement with the previous analysis,[13] and there are 30 distinct minima. The connectivity is actually easier to describe for the direct octahedron to octahedron rearrangements that occur for $\rho_0 < 4.1$, as discussed below. The tunneling splittings with degeneracies in parentheses are $8\beta(1)$, $2\beta(15)$, $-2\beta(9)$, and $-4\beta(5)$, and the reaction graph therefore contains odd-membered rings. In this case the MS group analysis takes about 10 min of cpu time on a Sun SPARCstation 10/41; there are 22 classes with 1 (twice), 15 (four times), 40 (four times), 45 (twice), 90 (four times), 120 (four times), and 144 (twice) members. There is one accidental

(54) Berry, R. S.; Braier, P.; Hinde, R. J.; Cheng, H.-P. *Isr. J. Chem.* **1990**, *30*, 39.

(55) Huber, K. P.; Herzberg, G. *Constants of Diatomic Molecules*; Van Nostrand Reinhold: New York, 1979.

(56) The numerical values were obtained for well depths of 0.000 3863/0.000 074 24 hartree and equilibrium pair separations of 3.8/1.76 Å for Ar/Ne both here and for the Lennard-Jones clusters.

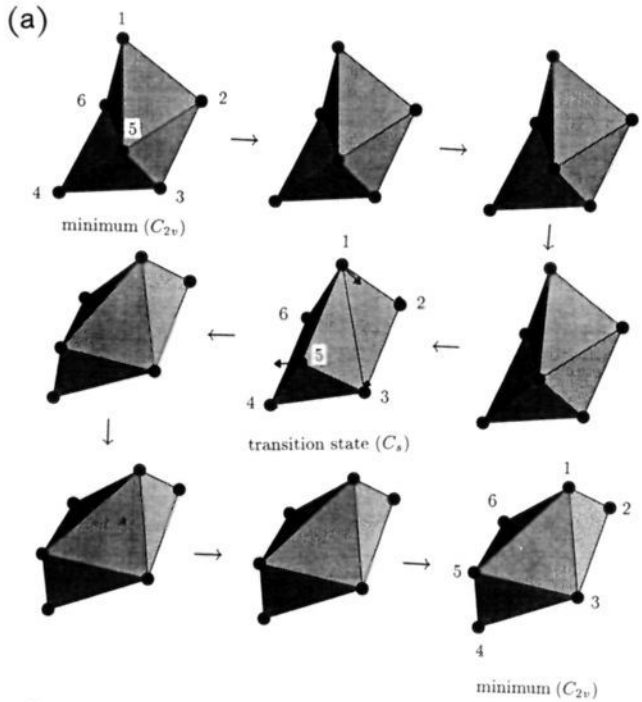

Figure 6. Degenerate rearrangements of the M_6 incomplete pentagonal bipyramid calculated at $\rho_0 = 6$: (a, top) DSD process via a capped square-based pyramid, (b, bottom) edge-bridging process via an edge-bridged pentagonal bipyramid.

degeneracy in the above tunneling levels: the 15 states at energy 2β span a ten- plus a five-dimensional irreducible representation, and the only allowed transition is between the latter states and the five states at -4β, with an energy of 6β.

The situation is simpler when the potential is longer-ranged. For $1.9 \leq \rho_0 \leq 4.1$ the octahedron rearranges directly via a CSBP, as shown in Figure 7. The calculated pathway for $\rho_0 = 4$ has 37 steps and the barrier is 0.000 42/0.000 081 hartree for Ar/Ne. Hence, $S = 4.257\ a_0$, $\gamma = 1.01$, $\gamma_m = 237.5$ amu, $D = 2.510\ a_0$, and $\beta = -7.9 \times 10^{-12}$ cm^{-1} for Ar and $S = 1.960\ a_0$, $\gamma = 1.01$, $\gamma_m = 118.5$ amu, $D = 1.155\ a_0$, and $\beta = 0.059$ cm^{-1} for Ne. Note that this rearrangement is almost completely delocalized, with $\gamma \approx 1$. For the labeling scheme of Figure 7, the generator is

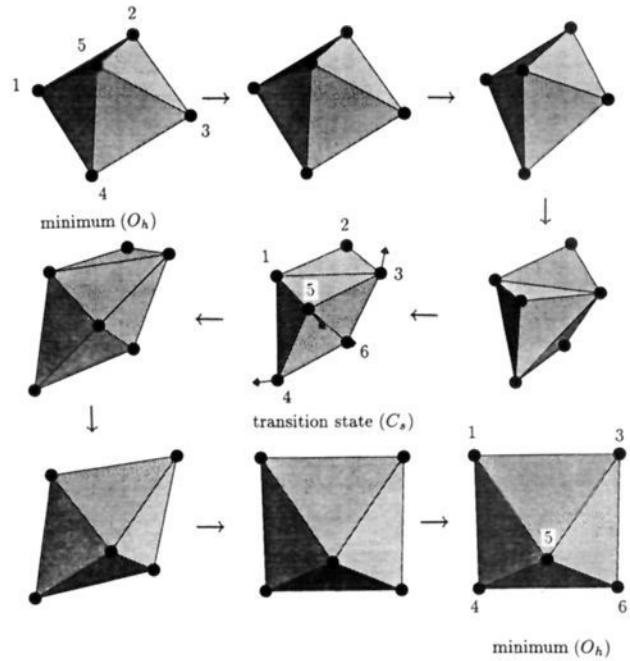

Figure 7. Degenerate rearrangement of the M_6 octahedron via a capped square-based pyramid calculated at $\rho_0 = 4$.

(36)(45)*. This is equivalent to the generator used above, and so the MS group, splitting pattern, etc. are also the same.

The reaction graph is again 8-fold connected, and each pair of adjacent octahedra are linked by three distinct versions of the CSBP transition state; such a possibility has in fact been previously considered by Bone in an abstract example.[41] This 8-fold connectivity is the largest found in the present study, and it is interesting to compare the tunneling splittings with those expected for the "complete graph"[57] where every minimum would be directly connected to every other distinct minimum. In this case it is easy to show that, within the present approximation, there would be one nondegenerate level at $n\beta$, where n is the number of distinct minima, and an $(n-1)$-fold degenerate set of levels at $-\beta$. The actual splitting pattern, with only four distinct energies and a largest eigenvalue of 8β, is clearly approaching this limit.

For $\rho_0 < 1.9$ the mechanism changes and the lowest energy rearrangement of the octahedron proceeds via a D_{3h} trigonal prism, which may be viewed as the limiting geometry of the CSBP. For the labeling scheme of Figure 8, the generator is (12)(46)*, and so the MS group, splitting pattern, etc. are the same as for the previous two cases. The reaction pathway consisted of 23 steps with barriers of 0.000 050/0.000 0096 hartree for Ar/Ne, giving $S = 10.686\ a_0$, $\gamma = 1.00$, $\gamma_m = 240.0$ amu, $D = 9.400\ a_0$, and $\beta = -1.0 \times 10^{-11}$ cm^{-1} for Ar and $S = 4.974\ a_0$, $\gamma = 1.00$, $\gamma_m = 120.0$ amu, $D = 4.375\ a_0$, and $\beta = 0.061$ cm^{-1} for Ne. Note that in this case the mechanism is completely delocalized and γ_m is the total molecular mass.

$[LJ]_3$ and $[LJ]_4$. The case of the Lennard-Jones cluster $[LJ]_3$ is somewhat unusual because there is only one distinct version of the equilateral triangular minimum.[18] This minimum is linked to itself by three distinct linear transition states, and although there cannot therefore be any tunneling splittings, we may still calculate β from the formulas in section III for comparison with $[LJ]_4$. The reaction path in this case has 39 steps, and the barrier is 0.000 37/0.000 074 hartree for Ar/Ne, giving $S = 16.273\ a_0$, $\gamma = 1.50$, $\gamma_m = 80.0$ amu, $D = 10.295\ a_0$, and $\beta = -8.2 \times 10^{-26}$ cm^{-1} for Ar and $S = 7.434\ a_0$, $\gamma = 1.50$, $\gamma_m = 40.0$ amu, $D =$

(57) See e.g.: Chartrand, G. *Introductory Graph Theory*; Dover: New York, 1985. Mezey, P. G. *Studies in Theoretical Chemistry: Potential Energy Hypersurfaces*; Elsevier: Amsterdam, 1987.

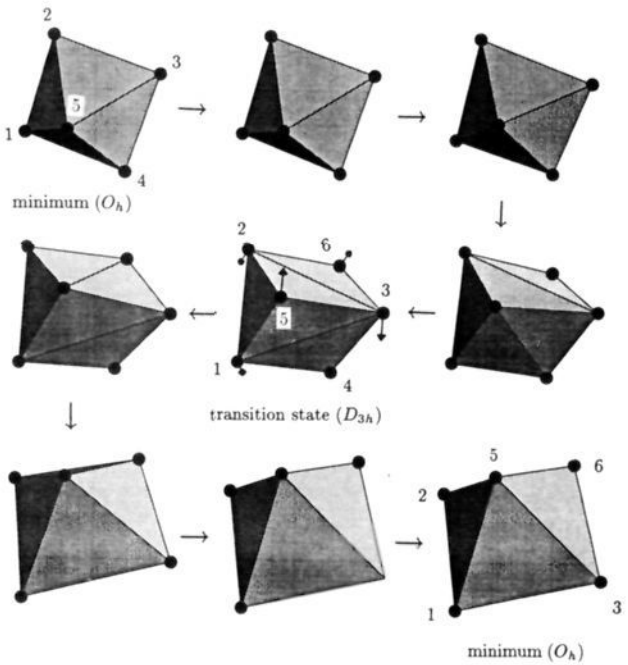

Figure 8. Degenerate rearrangement of the M_6 octahedron via a D_{3h} trigonal prism calculated at $\rho_0 = 1$.

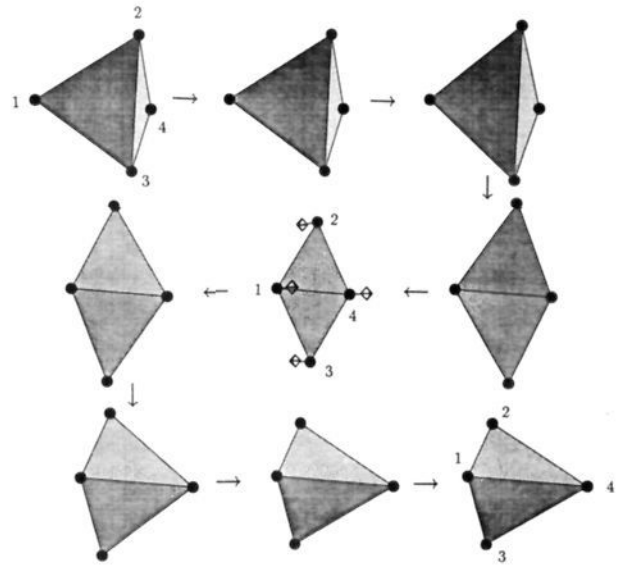

Figure 9. Rearrangement of the $[LJ]_4$ tetrahedron via a planar D_{2h} transition state.

4.768 a_0, and $\beta = -0.000\ 16\ cm^{-1}$ for Ne. The generator is (12) and $h_{CNPI} = h_{MS} = 12$.

$[LJ]_4$ is more interesting; the global minimum tetrahedron ($E = -6\ \epsilon$) can rearrange via an edge-bridging-type process with a planar D_{2h} transition state ($E = -5.073\ 421\ \epsilon$), as shown in Figure 9. The pathway has 34 frames, and the barrier is 0.000 36/0.000 069 hartree for Ar/Ne, so $S = 26.797\ a_0$, $\gamma = 1.00$, $\gamma_m = 160.0$ amu, $D = 10.155\ a_0$, and $\beta = 2.4 \times 10^{-33}\ cm^{-1}$ for Ar and $S = 12.411\ a_0$, $\gamma = 1.00$, $\gamma_m = 80.0$ amu, $D = 4.704\ a_0$, and $\beta = -5.8 \times 10^{-6}\ cm^{-1}$ for Ne. Hence, this rearrangement is completely delocalized. The generator for the labeling scheme in Figure 9 is $(14)(23)^*$, $h_{CNPI} = h_{MS} = 48$, and there are two distinct minima which are linked by this rearrangement. Furthermore, the MS group is isomorphic to O_h, with E^* corresponding to the point group inversion operator, i, and the dipole moment operator therefore transforming as A_{1u}. The tunneling

Table I. Lennard-Jones Parameter Values Employed for Benzene–Ar_1 and Benzene–Ar_2

atoms	ϵ/hartree	σ/Å
C–Ar	1.211×10^{-4}	3.42
H–Ar	7.015×10^{-5}	3.21
Ar–Ar	3.787×10^{-4}	3.448

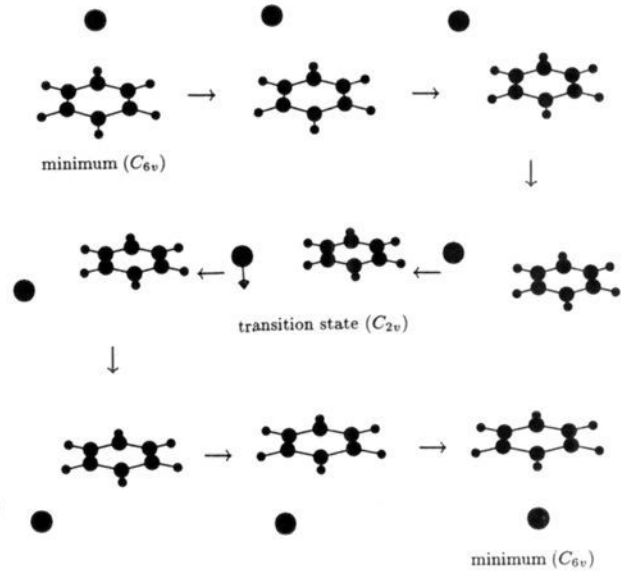

Figure 10. Rearrangment of benzene–Ar_1 via a C_{2v} transition state.

states are A_{1g} at energy β and A_{2u} at $-\beta$, and electric dipole transitions are therefore forbidden between them.

Benzene–Ar_1 and Benzene–Ar_2. In a previous study[17] it was found that benzene–Ar_2, for example, possesses some very facile rearrangements which might be expected to produce observable tunneling splittings. The potential used in the present calculations has atom–atom Lennard-Jones dispersion–repulsion terms and includes a first-order approximation to the induction energy[17] based upon a distributed multipole analysis.[58] The Lennard-Jones parameters are given in Table I; the C–Ar and H–Ar ϵ parameters were produced using the Slater–Kirkwood combination scheme[59] (geometric means) and are used in preference to the parameters employed by Ondrechen *et al.*,[60] as they appear to give a better binding energy for benzene–Ar_1.[61] The different parameters result in a change in geometry of one of the transition states of benzene–Ar_2 from C_{2v} to C_s, as discussed below. The reaction pathways were all calculated for a fixed benzene molecule, as before,[17] which means that they are further idealized. The optimizations were conducted in Cartesian coordinates[19,20] and converged rapidly, in contrast to previous calculations using internal coordinates.[17] In this case the second derivatives were formed from two-sided numerical derivatives of the analytic gradient.[17]

The generator for the rearrangement of benzene–Ar_1 shown in Figure 10 is E^*. The C_{6v} minimum and C_{2v} transition state have energies of 0.001 1072 and 0.000 4219 hartree, respectively, and the Ar atom lies 3.470/5.318 Å from the center of the ring. The reaction path consisted of 149 steps, and with the barrier of 0.000 6853 hartree, we find $S = 27.722\ a_0$, $\gamma = 1.00$, $\gamma_m = 40.0$ amu, $D = 13.298\ a_0$, and $\beta = 1.6 \times 10^{-31}\ cm^{-1}$. In this case $h_{CNPI} = 2 \times (6!)^2$ and the MS group has the same class structure as the point group D_{6h}, with 24 members and the dipole moment

(58) Stone, A. J. *Chem. Phys. Lett.* **1981**, *83*, 233. Stone, A. J.; Alderton, M. *Mol. Phys.* **1985**, *56*, 1047. Stone, A. J. In *Theoretical Models of Chemical Bonding*; Maksić, Z. B., Ed.; Springer-Verlag: Berlin, 1991; part 4.
(59) Slater, J. C.; Kirkwood, F. G. *Phys. Rev.* **1931**, *37*, 682.
(60) Ondrechen, M. J.; Berkovitch-Yellin, Z.; Jortner, J. *J. Am. Chem. Soc.* **1981**, *103*, 6586.
(61) Menapace, J. A.; Bernstein, E. R. *J. Phys. Chem.* **1987**, *91*, 2533.

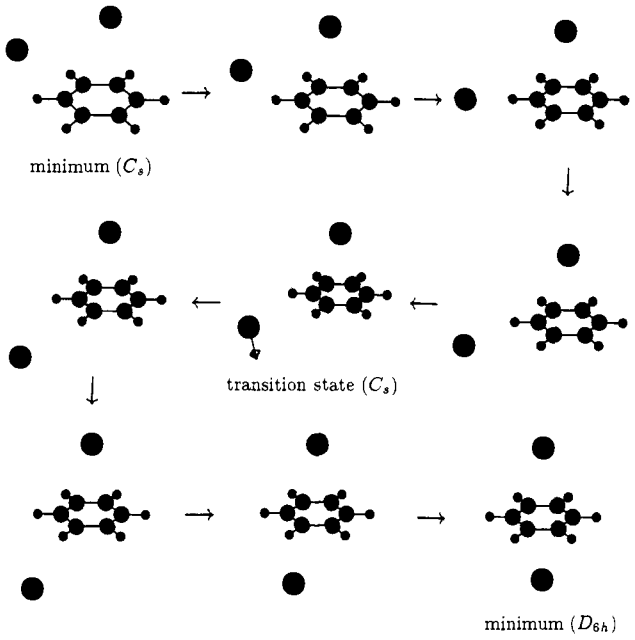

Figure 11. Rearrangement of the (2 + 0) minimum of benzene–Ar_2 to the (1 + 1) global minimum.

operator transforming as A_{1u}. There are 86 400 distinct minima linked in pairs, and the two tunneling states are A_{1g} at energy β and A_{2u} at $-\beta$; the electric dipole transition between these two levels is therefore forbidden.

For benzene–Ar_2 there are two minima: the (2 + 0) C_s minimum has both Ar atoms on the same face of the ring and the (1 + 1) D_{6h} minimum has one on each—the energies for the current potential are 0.002 0699 and 0.002 237 hartree, respectively. A relatively high energy transition state links the two, as shown in Figure 11; the barriers are 0.000 50 and 0.000 67 hartree, and the reaction path has 107 steps, giving S = 21.277 a_0, γ = 1.99, γ_m = 40.19 amu, D = 13.830 a_0, and $\beta = 3.1 \times 10^{-30}$ cm^{-1}. Hence, the migration of atoms between faces is unlikely to produce any detectable splitting effects in either benzene–Ar_1 or benzene–Ar_2. However, there are two distinct degenerate rearrangements of the (2 + 0) minimum with much lower barriers. The transition states have C_{2v} (Figure 12a) and C_s (Figure 12b) symmetry with energies of 0.002 0024 and 0.001 9915 hartree and barriers of 0.000 065 and 0.000 075 hartree, respectively. For the lower energy transition state, the reaction pathway has 45 steps and S = 8.673 a_0, γ = 1.00, γ_m = 80.0 amu, D = 8.317 a_0, and $\beta = -1.2 \times 10^{-9}$ cm^{-1}. Note that in the fixed benzene approximation this rearrangement is completely delocalized. The transition state of higher energy correlates with a more symmetrical C_{2v} structure when the Lennard-Jones parameters of Ondrechen *et al.*[60] are used. The reaction path for the present potential has 51 steps and S = 6.988 a_0, γ = 1.96, γ_m = 40.86 amu, D = 6.515 a_0, and $\beta = -4.0 \times 10^{-6}$ cm^{-1}.

Hence, for the degenerate rearrangements of the (2 + 0) minimum, we calculate a somewhat larger tunneling splitting for the mechanism with the higher barrier; the latter process is more localized, and so the estimated effective mass is lower. The cooperativity of the two rearrangements can also be seen from the displacements along the reaction path shown in Figure 12.

For the labeling schemes in the figure, the appropriate generators are (AB)(26)(35)* and (13)(46)*, corresponding to the C_{2v} and C_s transition states, respectively. Each rearrangement on its own gives rise to an MS group with 12 members and a connectivity of 2. Since $h_{CNPI} = 2 \times 2! \times (6!)^2$, the distinct (2 + 0) minima are linked in 172 800 disconnected sets with six members each, connected in a ring. The MS group is isomorphic to C_{6v} with the dipole moment operator transforming as A_2. The

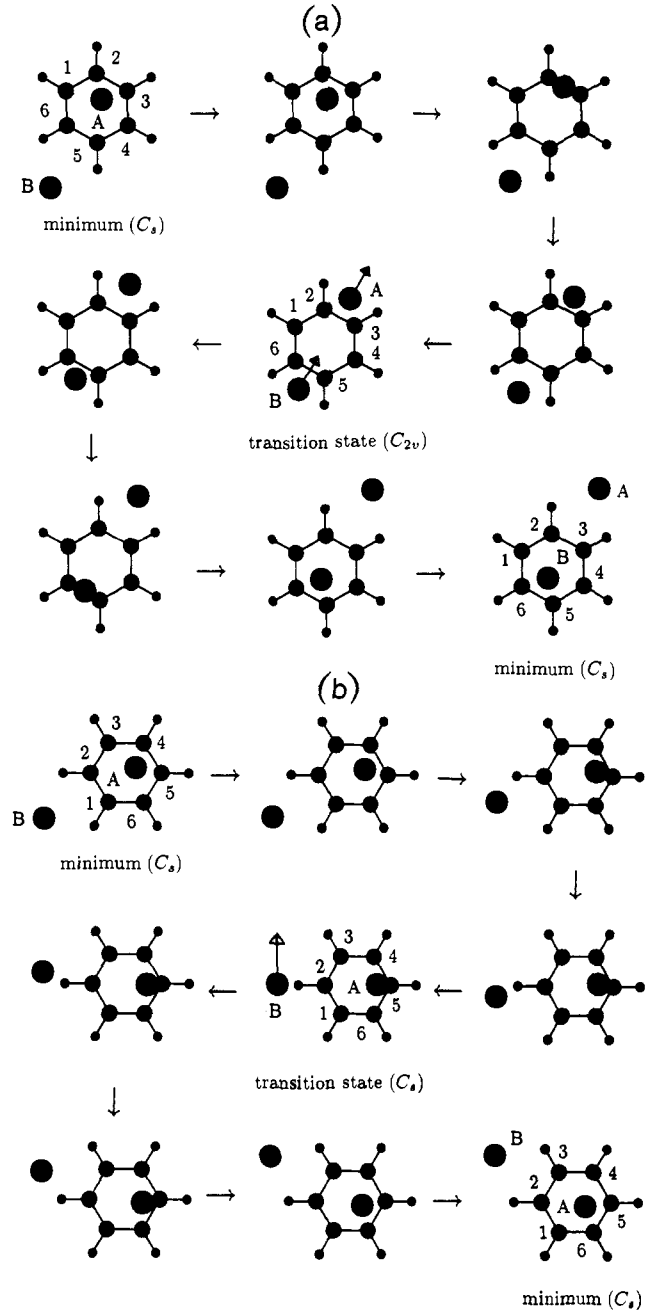

Figure 12. Degenerate rearrangements of the (2 + 0) minimum for benzene–Ar_2 via (a, top) C_{2v} and (b, bottom) C_s transition states. These are overhead views; the height of the two Ar atoms above the ring does not vary greatly throughout both processes.

splitting pattern, appropriately enough, is the same as for the π system of benzene, because the present tunneling problem generates the same secular determinant as the simplest Hückel treatment of this molecule. Using the labels of C_{6v}, we find the tunneling states $A_1(2\beta)$, $E_1(\beta)$, $E_2(-\beta)$, $B_1(-2\beta)$, and electric dipole transitions are forbidden within this manifold.

When the two rearrangements are considered together, the MS group increases to 24 operations with a connectivity of 4 and a class structure isomorphic to D_{6h}, where interchange of the two argon atoms (AB) corresponds to the point group operator i. This is the largest MS group possible if the two argon atoms are confined to one side of the benzene ring. The distinct minima occur in 86 400 disconnected sets with 12 in each. Using the appropriate labels for D_{6h}, the dipole moment operator transforms as A_{2g} and the tunneling states are $A_{1g}(2\beta_b + 2\beta_a)$, $A_{2u}(2\beta_b - 2\beta_a)$, $E_{1g}(\beta_b + \beta_a)$, $E_{1u}(\beta_b - \beta_a)$, $E_{2u}(-\beta_b + \beta_a)$, $E_{2g}(-\beta_b - \beta_a)$, $B_{1u}(-2\beta_b + 2\beta_a)$, and $B_{1g}(-2\beta_b - 2\beta_a)$, where β_b corresponds to the rearrangement

in Figure 12b, etc., and again no electric dipole transitions are allowed within this manifold. The effective values of β are now $\beta_a = -1.4 \times 10^{-9}$ and $\beta_b = -6.4 \times 10^{-6}$ cm^{-1}. As the mirror relation for the energies is maintained, we may also conclude that there can be no odd-membered rings in the reaction graph.

VI. Conclusions

Tunneling splittings have been predicted for a range of model cluster systems, including both an analysis of the reaction graph and an estimate of the probable magnitude of the effect in each case. The connectivity of the reaction graph is calculated automatically, given a minimal number of generator operations, and is used to set up the corresponding secular determinant for a linear combination of localized wave functions approximation to the tunneling states. A Hückel-type approach is employed in which only the off-diagonal Hamiltonian matrix elements between minima that are directly linked by a given rearrangement are needed. These are estimated by mapping the many-dimensional reaction pathway onto a model one-dimensional problem, and calculations for both degenerate and nondegenerate rearrangements are possible. The data required are all obtained from the calculated minimum-energy reaction pathways in the form of the barrier, the distance between the two minima in nuclear configuration space, and an effective mass.

Ab initio results at the DZP/MP2 level for the trans-tunneling pathway of $(HF)_2$ give an estimate for the tunneling splitting that is in error by between 1 and 2 orders of magnitude compared to experiment and accurate calculations. Hence, the present procedure should be capable of indicating which clusters are likely to show significant tunneling effects and provide the splitting pattern and an estimate of the associated magnitudes. The allowed electric dipole transitions within a given manifold are also generated automatically.

For $C_5H_5^+$ the splitting pattern agrees with a previous analysis, and one ambiguity in the assignment of symmetry labels has been resolved. However, in both this system and $B_8H_8^{2-}$ the tunneling splittings are probably too small to be seen experimentally. Significant effects are predicted for model clusters bound by Lennard-Jones and Morse potentials, especially for a light element such as Ne. Observable splittings are also calculated for the (2 + 0) isomer of benzene–Ar_2 due to the two low-energy degenerate rearrangements of the two Ar atoms on one face of the benzene ring.

Acknowledgments. The author is a Royal Society University Research Fellow. This project was initially prompted by a stimulating seminar given at the University of Cambridge in February 1993 by Prof. R. J. Saykally and was subsequently encouraged by Prof. N. C. Handy, who provided helpful advice concerning the multiminima perturbation problem. Thanks are also due to Dr. R. G. A. Bone for his useful suggestions, especially concerning the MS group, and to Prof. R. S. Berry for his additional comments. Some of the calculations were made possible thanks to a grant of supercomputer time from the SERC.

Appendix

The estimate of the effective mass described in section III is certainly not unique. A plausible alternative would be to calculate this quantity from the energy change resulting when the transition state is perturbed slightly along the minimum-energy reaction path. This is attractive because, in the semiclassical approach, β is defined as an integral over the classically forbidden region,[2] which is centered on the transition state in a degenerate rearrangement. However, there remains the problem of mapping the pathway onto a one-dimensional function of the path length, s.

If all the atoms have the same mass, m, then it is not hard to show that $\Delta s^2 = m\Delta q^2$, where Δq is the magnitude of the normal-mode displacement for the unique degree of freedom with negative curvature. This suggests that the appropriate Hamiltonian is

$$\hat{H} = -\frac{1}{2}\frac{\partial^2}{\partial q^2} + \frac{1}{2}\left(\frac{\partial^2 E}{\partial q^2}\right)_{ts} q^2 \equiv -\frac{1}{2m}\frac{\partial^2}{\partial s^2} + \frac{1}{2}m\left(\frac{\partial^2 E}{\partial q^2}\right)_{ts} s^2$$

and that the effective mass be defined as $(\partial^2 E/\partial s^2)_{ts}/(\partial^2 E/\partial q^2)_{ts}$.

All the splittings reported in section V (and for the water trimer) were recalculated using the above estimate of the effective mass, which was usually found to be less than or equal to γ_m. The new splittings are generally larger than before; for example, $\beta = 2.2$ cm^{-1} for $(HF)_2$, which is now too big. However, the only case where a previously negligible splitting may become significant is for $C_5H_5^+$, where β increases to the order of 10^{-5} cm^{-1}.